Diffusion–annihilation processes in weighted scale-free networks with an identical degree sequence

J. Stat. Mech. (2011) P10001

(http://iopscience.iop.org/1742-5468/2011/10/P10001)

Journal of Statistical Mechanics: Theory and Experiment
An IOP and SISSA journal

Diffusion–annihilation processes in weighted scale-free networks with an identical degree sequence

Yichao Zhang[1], **Zhongzhi Zhang**[2,3], **Jihong Guan**[1] **and Shuigeng Zhou**[2,3]

[1] Department of Computer Science and Technology, Tongji University, 4800 Cao'an Road, 201804, Shanghai, People's Republic of China
[2] School of Computer Science, Fudan University, 200433, Shanghai, People's Republic of China
[3] Shanghai Key Lab of Intelligent Information Processing, Fudan University, 200433, Shanghai, People's Republic of China
E-mail: 2008zhangyichao@tongji.edu.cn, zhangzz@fudan.edu.cn, jhguan@tongji.edu.cn and sgzhou@fudan.edu.cn

Received 13 April 2011
Accepted 3 September 2011
Published 5 October 2011

Online at stacks.iop.org/JSTAT/2011/P10001
doi:10.1088/1742-5468/2011/10/P10001

Abstract. $A+A \to \emptyset$ and $A+B \to \emptyset$ diffusion–annihilation processes have so far been studied on weighted uncorrelated scale-free networks and fractal scale-free networks. In the previous reports it was widely accepted that the segregation of particles in the processes is introduced by the fractal structure. In this paper we study these processes on a family of weighted scale-free networks with an identical degree sequence. We find that the depletion zone and segregation are essentially caused by disassortative mixing, namely, high-degree nodes tend to connect with low-degree nodes. Their influence on the processes is governed by the correlation between the weight and degree. Our finding suggests that the weight and degree distribution do not suffice to characterize the diffusion–annihilation processes on weighted scale-free networks.

Keywords: disordered systems (theory), network dynamics

Contents

1. Introduction

Complex networks are a powerful and versatile mathematical tool for representing and modeling the structure of complex systems [1, 2]. Their wide applications in distinct areas have made them an area of much research in the past decade [3, 4]. Prompted by data mining and the increased computing power of computers, extensive empirical studies have unveiled that most real networked systems can be characterized by a power-law degree distribution $P(k) \sim k^{-\gamma}$. This observation has led to an increase in research on the disordered organization of real-world systems [1]–[4]. The characteristic exponent γ, usually observed in the range $\in (2, 3]$ in recent empirical studies [1]–[4], is very important since it fundamentally influences some dynamical processes of the scale-free networks, e.g. synchronization [5, 6], the spread of diseases [7], and so forth. Among these processes, one aspect that has recently received considerable attention is the diffusion–annihilation problem, i.e. bimolecular chemical and physical reactions of the identical particles $A + A \to \emptyset$ and different particles $A + B \to \emptyset$ [8]–[16].

Unlike diffusion–reaction, the substances in diffusion–annihilation processes do not yield products with mass. In the study of diffusion–annihilation, the density ρ of the surviving particles is thus a crucial problem since it presents a quantitative description of the reaction process. In the long time limit, ρ behaves as

$$\frac{1}{\rho(t)} - \frac{1}{\rho(0)} = kt^f, \tag{1}$$

where k is the rate constant and $\rho(0)$ is the particle density at $t = 0$. In the mean-field approximation with $\rho_A(0) = \rho_B(0)$, both processes can be described as $\mathrm{d}\rho(t)/\mathrm{d}t = -\mathrm{const}\rho(t)^2$, whose solution is $f = 1$. The solution is valid in regular lattices of Euclidean space [12] with a spatial dimension $d > d_c$, where d_c is the critical dimension of this process. For the $A + A \to \emptyset$ process $d_c = 2$, while for the $A + B \to \emptyset$ process $d_c = 4$ [13].

J. Stat. Mech. (2011) P10001

Further studies on fractals found that the exponent $f = d_s/4$ for $A + B \to \emptyset$ [14], where d_s is the spectral dimension of the fractal structure.

As the existence of the depletion zone $A + A \to \emptyset$ [15] and segregation of the reactants $A + B \to \emptyset$ [16], the upper bound of the exponent f for the regular lattices is 1. Whereas, when the processes are performed on scale-free networks with identical nodes and links, f can be considerably higher than 1 [8]. Inspired by these observations, the relation between γ and f on $A+A \to \emptyset$ was investigated analytically [9] in uncorrelated scale-free networks [17, 18]. In essence, the term 'uncorrelated' denotes that no degree–degree correlations exist among nodes in the networks, namely, the conditional probability $P(k'|k)$ that a node of degree k is connected to a node of degree k' can be formalized as $k'P(k')/\langle k\rangle$. The analytical solution shows that f is only governed by the exponent γ for this class of scale-free networks. Subsequently, an interesting study of $A + B \to \emptyset$ on fractal scale-free networks shows that segregation can also be found in the scale-free networks [10]. Influenced by the segregation, the reaction process is apparently hampered.

Very recently, considering heterogeneous distributions of weights [19, 20], heuristic analytical research on the weighted uncorrelated scale-free networks has presented a more realistic conclusion [11]. In this work, the weight of links is defined as $w_{ij} = (k_i k_j)^\theta$ with the degree k_i and k_j of both nodes, where θ is the network's weight parameter which characterizes the dependence between link weight and the node degrees [19]. When $\theta = 0$, there is no dependence between link weight and node degree, all link weights equal one, and the network becomes an unweighted network. When $\theta > 0$ it is a weighted network where links have different weights. The larger θ gets, the wider the difference between links becomes. Based on the mean-field rate equation for the average density ρ_k of a node with degree k, for the $A + A \to \emptyset$ process, the authors showed

$$\rho \sim \begin{cases} t^{-1} & \theta < \frac{\gamma-3}{2} \\ t^{-(1+\theta)/(\gamma-\theta-2)} & \frac{\gamma-3}{2} \leq \theta < \gamma - 2 \\ \mathrm{e}^{-t} & \theta \geq \gamma - 2, \end{cases} \tag{2}$$

in asymptotically large networks. For the $A + B \to \emptyset$ process, inserting the mapping relation, they claimed

$$\rho \sim \begin{cases} t^{-1} & \theta < \frac{\gamma-3}{2} \\ (t \ln t)^{-1} & \theta = \frac{\gamma-3}{2} \\ t^{-1/(\gamma-\theta-2)} & \frac{\gamma-3}{2} < \theta < \gamma - 2. \end{cases} \tag{3}$$

It has been shown that f is only governed by the weight and degree distribution.

In this paper we study a family of weighted scale-free networks with an identical degree sequence (weighted IDS-SF networks) and find that the reaction processes are vastly different from the previous reports [8]–[11]. We briefly introduce weighted random diffusion in section 2. Section 3 is devoted to introducing the IDS-SF networks. In section 4, our extensive numerical simulations are compared with previous analytical results of the diffusion–annihilation processes running on top of the weighted uncorrelated scale-free networks [11]. Finally, our conclusions are presented in section 5. Our findings indicate that disassortative mixing of the nodes is the essential reason for generation of the depletion zone and segregation in this class of scale-free networks.

J. Stat. Mech. (2011) P10001

2. Weighted random diffusion

Before introducing the construction of the networks, we briefly introduce a general random walk on weighted networks to clarify the influence of high-degree nodes (hubs) on the weighted random diffusion on scale-free networks. A random walk is a mathematical formalization of a trajectory that consists of taking successive random steps. A familiar example is the random walk phenomenon in a liquid or gas, known as Brownian motion [21, 22]. Random walk is also a fundamental dynamic process of complex networks [23]. Random walk on networks has many practical applications, such as navigation and search of information on the world wide web and routing on the internet [24]–[28].

Let us consider a weighted random walker starting from node i at step $t = 0$ and denote $P_{im}(t)$ as the probability of finding the walker at node m at step t. The probability of finding the walker at node j at the next step is

$$P_{ij}(t+1) = \sum_{m} a_{mj} \Pi_{m\to j} P_{im}(t), \tag{4}$$

where a_{mj} is an element of the network's adjacent matrix.

In this case, we define the weight of a link between nodes i and j as

$$w_{ij} = w_{ji} = \begin{cases} 0 & \text{link } i-j \text{ does not exist} \\ (k_i k_j)^{\theta} & \text{link } i-j \text{ exists} \end{cases} \tag{5}$$

where k_i and k_j denote the degree of node i and j, respectively. On the other hand, the strength of node i is defined as

$$s_i = \sum_{j\in\Gamma(i)} w_{ij} = \sum_{j\in\Gamma(i)} (k_i k_j)^{\theta}. \tag{6}$$

Thus the probability $P_{ij}(t)$ for the walker to travel from node i to node j in t steps is

$$P_{ij}(t) = \sum_{m_1,\ldots,m_{t-1}} \frac{w_{im_1}}{s_i} \times \frac{w_{m_1m_2}}{s_{m_1}} \times \cdots \times \frac{w_{m_{t-1}j}}{s_{m_{t-1}}}. \tag{7}$$

In other words, $P_{ij}(t) = \sum_{m_1,\ldots,m_{t-1}} P_{im_1} P_{m_1m_2} \cdots P_{m_{t-1}j}$. Comparing the expressions for P_{ij} and P_{ji} one can see that $s_i P_{ij}(t) = s_j P_{ji}(t)$. This is a direct consequence of the undirected feature of the network. For the stationary solution, one obtains $P_i^{\infty} = s_i/Z$ with $Z = \sum_i s_i$. This means the higher the strength of a node, the more frequently it tends to be visited by a walker. Notably, for degree uncorrelated networks [29], s_i in the steady state scales with k_i as $s_i \sim k_i^{\theta+1}$ [20].

3. Scale-free networks with an identical degree sequence (IDS-SF networks)

Scale-free networks with an identical degree sequence are a common topic in complex networks, and offer researchers a platform to understand how the dynamical behavior is influenced by the degree heterogeneity of networks [30, 31]. As a class of these networks [32, 33], the construction of the present model is controlled by a parameter q [32, 33] as shown in figure 1, evolving in a recursive way. We denote the network after n

J. Stat. Mech. (2011) P10001

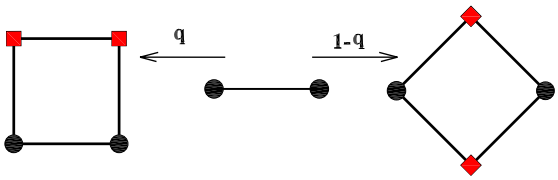

Figure 1. Iterative method of the network construction. Each edge is replaced by the connected clusters on the left-hand side with a certain probability q, otherwise by the one on the right-hand side, where red squares represent new nodes.

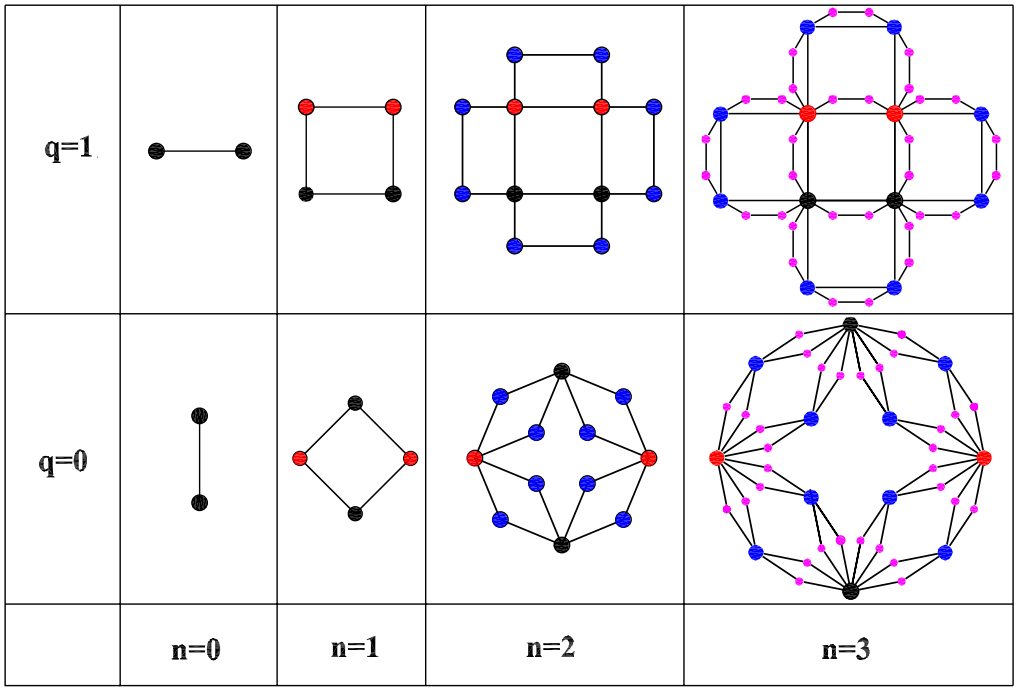

Figure 2. Illustration of the first three iterations of the network for the particular cases $q = 0$ and 1.

iterations by $G(n)$, $n \geq 0$. Then the networks are constructed as follows. For $n = 0$, the initial network $G(0)$ consists of two nodes connected to each other by a link. For $t \geq 1$, $G(n)$ is obtained from $G(n-1)$. That is to say, to obtain $G(n)$, one can add three links to each link existing in $G(n-1)$ (as shown on the left of figure 1) with probability q, or replace it with a quadrangle (as shown on the right of figure 1) with complementary probability $1-q$. In figure 2, we present the first three iterations of two special networks corresponding to two limiting cases $q = 0$ and $q = 1$, respectively.

Previous studies have shown that this class of scale-free networks exhibit a series of particular properties [32]. For instance, the same degree sequence independent of parameter q, identical degree distributions, and no triangles [3] formed by connections among the neighbors. In addition, the IDS-SF networks are disassortative for $q = 0$ (the index tends to -0.5 as $N \to \infty$ [34]) and uncorrelated for $q = 1$ [35]. As shown in figure 3, the Pearson coefficient increases by q from -0.15 to 0. Hence, for $q = 1$, the topological

J. Stat. Mech. (2011) P10001

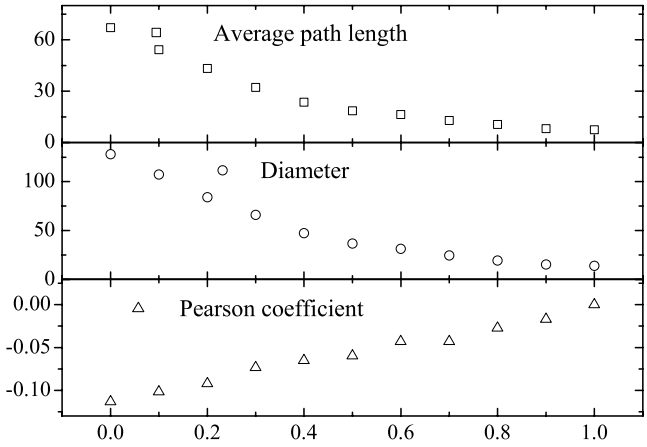

Figure 3. Pearson correlation coefficient, average path length, and diameter versus q ranging from 0 to 1 for IDS-SF networks. Each data point corresponds to ten independent realizations of the network for $n = 7$.

structure of the network satisfies the conditions of applying $P(k|k') = kP(k)/\langle k\rangle$ [11] and mean-field approximation. Also, the network is fractal for $q = 0$ and non-fractal for $q > 0$.

Influenced by these structural features, the dynamical processes on this class of scale-free network present a unique behavior. The behavior is distinct from that on the other scale-free networks, for instance the Barabási–Albert (BA) graph [9, 36] and uncorrelated configuration networks [9, 31]. In section 4, we will show the differences in the diffusion–annihilation processes.

4. Diffusion–annihilation processes on weighted IDS-SF networks

In section 2, we showed that $P_i^{\infty} = k_i^{\theta+1}/\Sigma_i k_i^{\theta+1}$. For $\theta > 0$, one can find that particles move toward hubs over time. Considering that hubs are the minority of the population, moving to them means becoming centralized. At these hubs, particles thus have a high probability of colliding and reacting with each other. This structural feature accelerates the reaction processes, differing scale-free networks from homogeneous networks [9]. Instead, for $\theta < 0$, the particles are repelled by the hubs. In this case, the particles become dispersed on the low-degree nodes (leaves) with time. Accordingly, the reaction rate of diffusion–annihilation tends to decrease with θ for the two processes. In what follows, we will show that the diffusion tendency mentioned above is correct, but the influence of θ on the reaction rate is not monotonic. The influence depends not only on degree distribution but also on other topological features.

We first generate a special IDS-SF structure in an iterative way with $n = 7$. The simulation results are obtained on IDS-SF networks with 10 924 nodes and 16 384 links. For the two reaction processes, each node in the networks can host at most one particle. The concrete processes are defined as follows: an arbitrary particle jumps with a certain probability w_{ij}/s_i from a node i to a randomly chosen nearest neighbor j. If it is empty, the particle fills it, leaving i empty. If j is occupied, the two particles annihilate, leaving both nodes empty. An initial fraction $\rho(0)$ of nodes in the networks is randomly chosen,

J. Stat. Mech. (2011) P10001

and is occupied by an A particle with probability 0.5 for both types. For the $A+B\to\emptyset$ process, the initial densities of A and B are equal, i.e. $\rho_B(0)=\rho_A(0)$. For a convenience of discussion, we define f as the first order derivative of $1/\rho(t)$, where $\rho(t)=\rho_A(t)$ for $A+A\to\emptyset$ and $\rho(t)=\rho_A(t)+\rho_B(t)$ for the $A+B\to\emptyset$ process. In the cases where $0<q<1$, each plot corresponds to 100 simulations that are 10 runs for 10 independent realizations of the network with the same parameters. For the two limiting cases $q=0,1$, each plot corresponds to 100 runs for the two deterministic networks.

As the degree sequences of the IDS-SF networks with $q\in[0,1]$ are the same, in which $\gamma=3$ [32], equations (2) and (3) can be rewritten as

$$\rho\sim\begin{cases}t^{-1} & \theta<0\\ t^{-(1+\theta)/(1-\theta)} & 0\le\theta<1\\ \mathrm{e}^{-t} & \theta\ge 1.\end{cases}\tag{8}$$

For the $A+B\to\emptyset$ process, inserting $\gamma=3$, one can also obtain

$$\rho\sim\begin{cases}t^{-1} & \theta<0\\ (t\ln t)^{-1} & \theta=0\\ t^{-1/(1-\theta)} & 0<\theta<1.\end{cases}\tag{9}$$

For convenience, we define two quantities as follows:

$$Q_{AA}=\frac{N_{AA}(t)}{M(t)(M(t)-1)},\tag{10}$$

$$Q_{AB}=\frac{N_{AB}(t)}{M(t)(M(t)-1)},\tag{11}$$

where $N_{AA}(t)$ denotes the number of close contacts between two nodes with identical particles for the $A+A\to\emptyset$ process. $N_{AB}(t)$ denotes the number of contacts between the distinct particles for the $A+B\to\emptyset$ process at time t [37]. $M(t)$ denotes the total number of particles at time t.

4.1. Case of $q=1$

As shown in figure 2, in the case $q=1$, the networks are reduced to the $(1,3)$-flower proposed in [34]. By definition [38], the fractal dimension d_{f} can be obtained by

$$d_{\mathrm{f}}=\lim_{n\to\infty}\left(\frac{\ln N_n}{\ln l_n}\right),\tag{12}$$

where N_n and l_n are the size and diameter, respectively, of G_n. Inserting $N_n=\frac{2}{3}(4^n+2)$ and $l_n=2n$ [34] into equation (12), we have

$$d_{\mathrm{f}}=\lim_{n\to\infty}(3\ln 2n).\tag{13}$$

Obviously, the net is infinite-dimensional, namely, a non-fractal network. For $A+A\to\emptyset$, figure 4(a) shows (I) ρ, (II) f, (III) Q versus time t for $\theta=-1,0,1$ on a double-logarithmic scale. The plots are logarithmically binned. In panels (a) and (b)-(II),

J. Stat. Mech. (2011) P10001

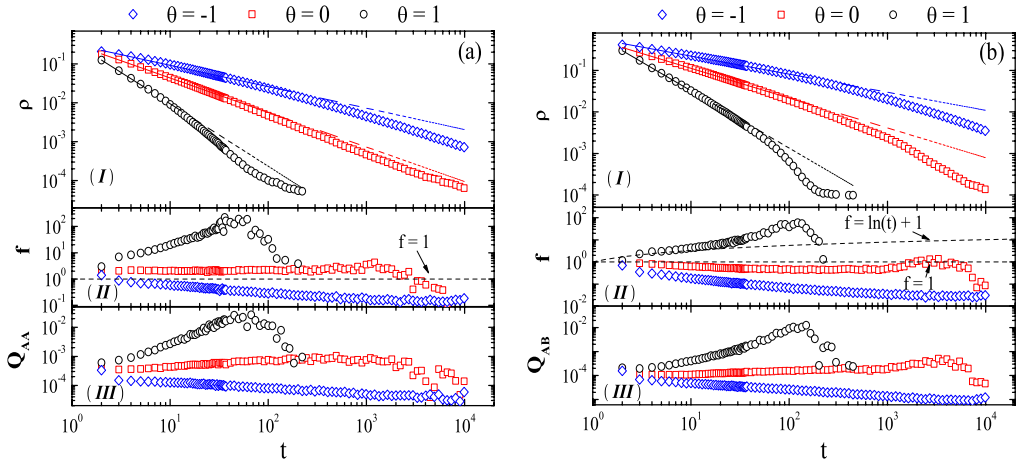

Figure 4. ρ, f and Q versus time t for (a) $A + A \to \emptyset$ and (b) $A + B \to \emptyset$ with $q = 1$. In panel (a)-(I), the dashed lines have slopes of $-0.55, -0.89$, and -1.61; in panel (b)-(I), they have slopes of $-0.44, -0.72$, and -1.38 from top to bottom. In panels (a) and (b)-(II), the dashed line corresponds to the mean-field prediction: for the $A + A \to \emptyset$ process, $f = 1$ when $\theta = 0, -1$, and $f = \exp(t)$ when $\theta = 1$; for $A + B \to \emptyset$, $f = 1$ when $\theta = -1$ and $f = \ln(t) + 1$ when $\theta = 0$.

$f_{t_{i+1}} = (1/\rho(t_{i+1}) - 1/\rho(t_i))/(t_{i+1} - t_i)$, ($i$ is a positive integer). In panels (a) and (b)-(III), $Q_{t_{i+1}} = (Q_{t_{i+1}} - Q_{t_i})/(t_{i+1} - t_i)$. The time interval $\log(t_{i+1}) - \log(t_i) = 0.1$.

Compared with the mean-field prediction, our simulations exhibit a series of distinct behaviors. For $\theta \geq 1$, the mean-field prediction $f = \mathrm{e}^t$ is much higher than our simulation results. To show the plots clearly, we omit the dashed line $f = \mathrm{e}^t$ in the panel. This discrepancy is primarily caused by the approximation $N_g \to \infty$ in the mean-field derivation. In this condition, $\langle k^{1+\theta} \rangle \to \infty$, which simplifies the differential equation to a solvable status. For $0 < \theta < 1$, the approximation in the literature [11] omits the reaction running on the low-degree nodes, which causes the predicted reaction rate to be lower than our observation. For $\theta = 0$, in terms of the scale of f, our observations roughly match the mean-field prediction. Also, it is consistent with the previous conclusion on finite size effects, i.e. $1/\rho(t) \sim N^{(3-\gamma)/2}t$ for $\gamma \leq 3$ [9]. Nevertheless, the value of f shown in figure 4(a) is slightly higher than these solutions. This is due to the global mean first-passage time of random walks. The mean-field solution of the mean first-passage time is proportional to N_g [39] in a uncorrelated scale-free network, while it is proportional to $N_g^{\ln 3/\ln 4}$ on this $(1, 3)$-flower [33]. Thus, one can expect a larger deviation in the network with a larger population. For $\theta < 0$, our observation indicates that the scale of f is lower than the prediction [11]. This deviation is caused by the approximation in the Taylor expansion, where high-order terms are ignored at the beginning of the reaction.

For the $A+B \to \emptyset$ process, we measure the relation between the total particle density $\rho(t) = \rho_A(t) + \rho_B(t)$ and time t as shown in figure 4(b). Our observation exhibits similar behavior to $A + A \to \emptyset$. Based on the probability of collision between two identical particles being equal to that for distinct ones, one can find Q_{AB} in figure 4(b) is about half of the corresponding Q_{AA}. Thus, f in the $A + B \to \emptyset$ process is basically lower than that in the $A + A \to \emptyset$ process.

J. Stat. Mech. (2011) P10001

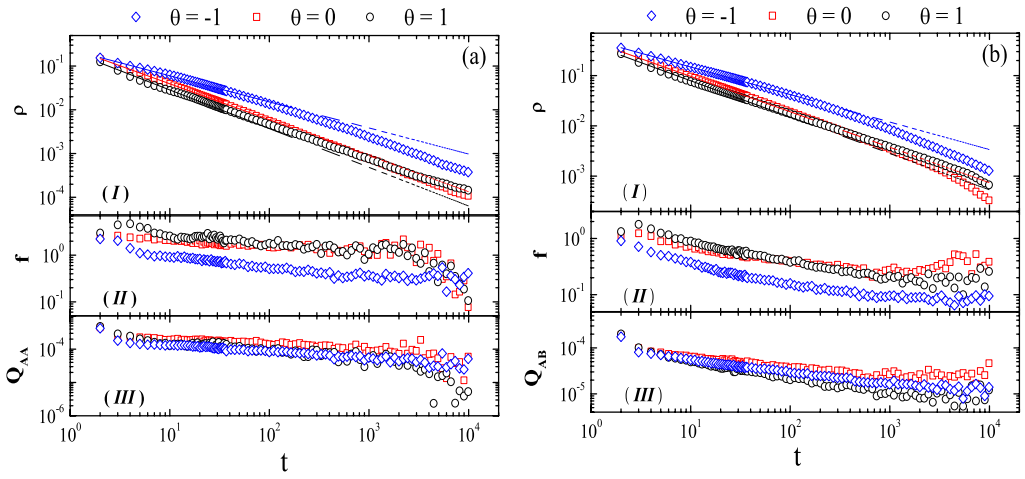

Figure 5. ρ, f and Q versus time t for (a) $A + A \to \emptyset$ and (b) $A + B \to \emptyset$ with $q = 0$. In panel (a)-(I), the dashed lines have slopes $-0.60, -0.82$, and -0.88; in panel (b)-(I), they have $-0.55, -0.70$, and -0.72 from the top to bottom.

It should be mentioned that the $(1, 3)$-flower is a network with a series of important properties, e.g. non-fractal topology, no degree correlations and scale-free degree distribution, satisfying the condition of mean-field approximation. Our simulations show that the annihilation processes for $\theta < 0$ can exhibit different behaviors from the previous reports. Thus, there is a need to provide such a complement to the previous discussion on both fractal scale-free networks [10] and weighted scale-free networks [11]. For integrity, we will investigate the other limiting case $q = 0$.

4.2. Case of $q = 0$

For $q = 0$, the networks are reduced to the $(2, 2)$-flower, which is a fractal network having fractal dimension $d_{\rm f} = \ln 4/\ln 2 = 2$ [34]. By definition, the fractal network is a network satisfying the fractal scaling $N_{\rm B}(l_{\rm B}) \sim l_{\rm B}^{d_{\rm f}}$, where $N_{\rm B}$ is the number of boxes needed to cover the entire network with boxes of size $l_{\rm B}$. On this network, hubs are located separately from each other [40, 41]. As is known, the mean-field theory can only be applied to the nets with infinite dimensionality [34, 10]. Thus, the discrepancies between the mean-field prediction and our results are not unexpected. However, the weighted networks have their unique subtle properties, which essentially influence the annihilation processes on them.

For the $A + A \to \emptyset$ process, figure 5(a) shows (I) ρ, (II) f, (III) Q_{AA} versus t for the set of θ on a double-logarithmic scale. The plots are also logarithmically binned. For $\theta = 1$, the exponent f decreases with t abnormally and exhibits contrary behavior to $q = 1$, in which f increases with t. Also, f in this case is generally equal to that for $\theta = 0$, while it is considerably higher than that for $\theta = 0$ and $q = 1$.

For the $A + B \to \emptyset$ process, figure 5(b) shows similar behavior to the $A + A \to \emptyset$ process. Because of $Q_{AA} \sim 2Q_{AB}$, f in this case is also much lower than the $A + A \to \emptyset$. Notably, for the unweighted case, i.e. $\theta = 0$, f is not the constant 0.5 mentioned in [10].

For homogeneous initial distributions with equal densities of A and B, $\rho_A(0) = \rho_B(0)$, local hubs and the random fluctuation in the initial particle number generate the

J. Stat. Mech. (2011) P10001

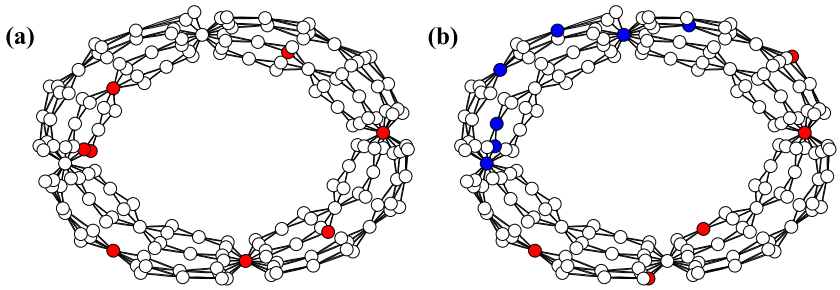

Figure 6. Illustration of the $A + A \to \emptyset$ and $A + B \to \emptyset$ processes on the IDS-SF networks with $n = 4$. (a) $A + A \to \emptyset$ at $t = 10$, and (b) $A + B \to \emptyset$ at $t = 15$. Red and blue plots denote A and B particles, respectively.

segregation of distinct particles, which drastically slows down the reaction rate. Usually, for unweighted uncorrelated scale-free networks it is hard for a large number of particles to adopt a close formation that cannot be penetrated by the other species because of a short diameter. However, for $q = 0$, the influence of disassortative mixing is strengthened by the high heterogeneous weight distribution as shown in figures 5(a) and (b). The influence can be treated as a hub attraction. The local hubs attract the particles more tightly the lower the diffusion rate is.

As shown in figure 6(a), a hub leads to a fast decay of the local A particle density in the beginning, followed by a slow decay in the long time regime as shown in figure 5(a). Thus, one can clearly observe depletion zones emerging from the intervals among hubs in this panel. In figure 5(b), a hub in a A- or B-rich domain can give rise to a pure A or B zone after a prompt local annihilation of A and B, leaving a relatively particle-free space among the hubs. With these segregations, one can observe a slow decay of the reaction rate, as shown in figure 5(b).

Interestingly, the depletion zone and segregation also inhibit particles moving from leaves to hubs when $\theta < 0$. The behavior can be observed by measuring the average degree of occupied nodes. Recalling the discussion at the beginning of this section, one can find that particles are attracted by the leaves in this condition. For $q = 1$, particles tend to agglomerate around hubs for $\theta > 0$ (see figure 7(a)) and around leaves for $\theta < 0$ (see figure 7(c)). Figure 7 is also logarithmically binned. Comparing figures 4(a) and (b)-(II) with figures 5(a) and (b)-(II), one can see that the depletion zone and segregation slow down the reaction rate for $\theta > 0$. For $\theta < 0$, comparing figure 4(b)-(II) with figure 5(b)-(II), instead, they accelerate the rate slightly. This is because they slow down the decentralizing process of the particles. For $\theta = 0$, figure 7(b) shows their influences are hardly noticed. Apparently, this behavior is distinct from the previously reported results [10, 11].

4.3. Case of $0 < q < 1$

For $0 < q < 1$, the networks are stochastic but not self-similar [33]. Thus the networks are non-fractal in this middle case. In order to discuss the variation in the dependence of f on q, we perform extensive numerical simulations for a set of q from 0 to 1. The simulation settings are the same as the former cases. When q is increasing from 0 to 1, the exponent of global mean first-passage time of random walks $G(N_g)$, decreases from 1

J. Stat. Mech. (2011) P10001

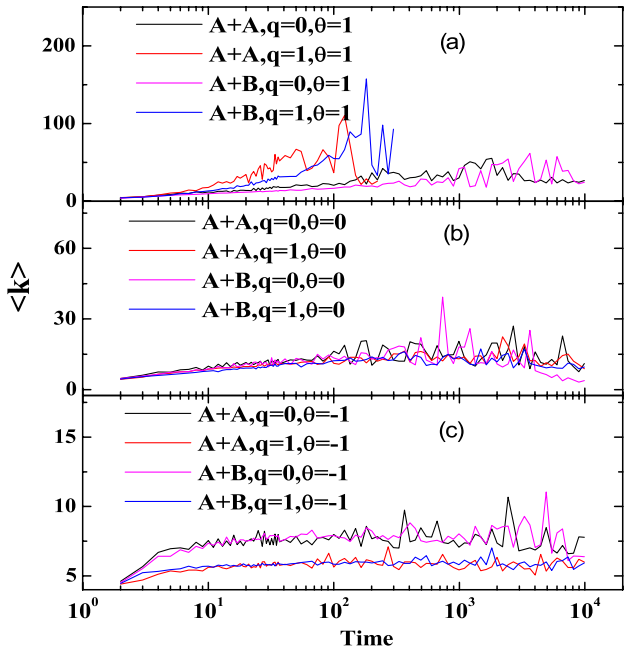

Figure 7. $\langle k\rangle$ as a function of time t for $A+A\to\emptyset$ and $A+B\to\emptyset$ for $\theta=-1,0,1$ with $q=0,1$ respectively.

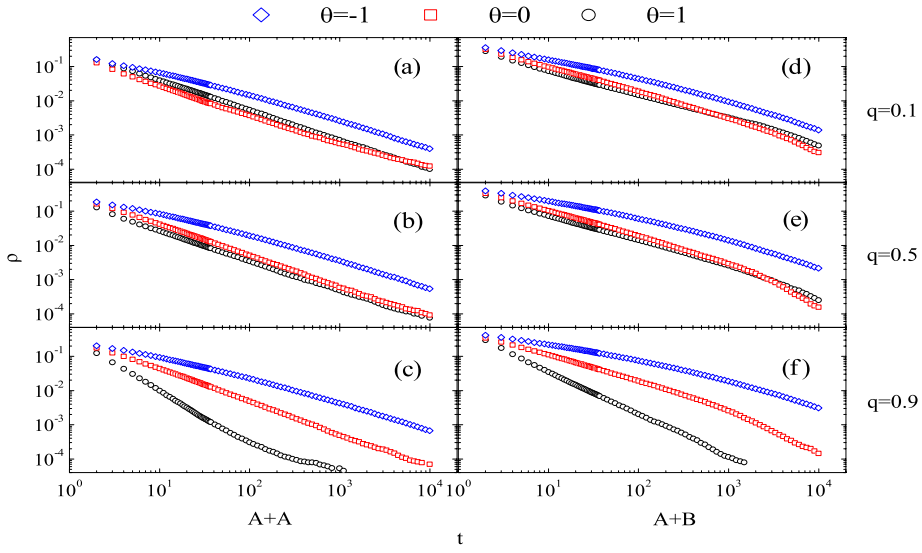

Figure 8. Particle density ρ as a function of time t with $\theta=-1,0,1$ on the IDSSF networks: (a) $q=0.1$, (b) $q=0.5$, (c) $q=0.9$ for the $A+A\to\emptyset$ processes; (d) $q=0.1$, (e) $q=0.5$, (f) $q=0.9$ for the $A+B\to\emptyset$ processes.

to $\ln 3/\ln 4$ [33]. This indicates the transporting efficiency is enhanced during the process. At the same time, the diameter of the networks decreases and the disassortative mixing feature disappears.

With the increase of q, the segregations among hubs disappear gradually and the diffusion rate increases drastically, leading to an apparent enhancement in the reaction rate for $\theta=1$. One can work out the enhancement by comparing figures 8(a)–(c). Notably,

in panel (b), the segregations for $\theta = 0$ are purely topological. Although their influence is not so apparent as in panel (a), they are still present. Comparing panel (a) with (c) (and (d) with (f)), the subtle influence of segregations on the reaction rate for $\theta = -1$ can be identified as well. One can find that the particle density ρ in (a) and (d) is lower than that in (c) and (f) basically. This indicates that the reaction rate decreases slightly with q, which is consistent with our observation in section 4.2.

5. Conclusion

In summary, we have investigated the diffusion–annihilation process on a family of weighted scale-free networks with an identical degree sequence (weighted IDS-SF networks), which is controlled by a parameter $q \in [0, 1]$. In this paper, the weight of links is defined as $w_{ij} = (k_i k_j)^\theta$ with the degree k_i and k_j of both nodes, where θ is the network's weight parameter. For convenience, we defined a kinetic exponent f as $\mathrm{d}(1/\rho(t))/\mathrm{d}t$, where $\rho(t) = \rho_A(t)$ for the $A + A \to \emptyset$ process and $\rho(t) = \rho_A(t) + \rho_B(t)$ for the $A + B \to \emptyset$ process. Based on the definition, we provide numerical results to characterize the relation between f and the reaction time t for the $A + A \to \emptyset$ and $A + B \to \emptyset$ bimolecular reactions.

One significant observation is that, in contrast to the commonly accepted conception that the depletion zone and segregation only exist in fractal networks, they can exist in the diffusion–annihilation process on the non-fractal networks as well. This feature in scale-free networks was not reported in previous studies. In fact, the depletion zone and segregation can both exist in fractal and non-fractal networks no matter whether they are weighted or not. We found that the segregation effect is essentially caused by disassortative mixing, i.e. high-degree nodes tend to connect with low-degree nodes. For the weighted networks, its influence on the particles diffusion is greatly strengthened by the weight heterogeneity. We have demonstrated that both degree and weight distribution do not suffice to characterize the diffusion–annihilation processes on weighted scale-free networks. Our observations suggest that care should be taken when making general statements about the diffusion–annihilation process in weighted scale-free networks.

Acknowledgments

We thank Tamas Jambor for useful discussions. This work was supported by National Natural Science Foundation of China (NSFC) under grants Nos. 60873040, 60873070, 61074119, and the Shuguang Program of Shanghai Municipal Education Commission and Shanghai Education Development Foundation.

References

[1] Albert R and Barabási A-L, 2002 *Rev. Mod. Phys.* **74** 47
[2] Dorogvtsev S N and Mendes J F F, 2002 *Adv. Phys.* **51** 1079
[3] Newman M E J, 2003 *SIAM Rev.* **45** 167
[4] Boccaletti S, Latora V, Moreno Y, Chavez M and Hwanga D-U, 2006 *Phys. Rep.* **424** 175
[5] Atay F M, Biyikoğlu T and Jost J, 2006 *IEEE Trans. Circuits Syst.* I **53** 92
[6] Hagberg A, Swart P J and Schult D A, 2006 *Phys. Rev.* E **74** 056116
[7] Eguíluz V M and Klemm K, 2002 *Phys. Rev. Lett.* **89** 108701
[8] Gallos L K and Argyrakis P, 2004 *Phys. Rev. Lett.* **92** 138301
[9] Catanzaro M, Boguñá M and Pastor-Satorras R, 2005 *Phys. Rev.* E **71** 056104

J. Stat. Mech. (2011) P10001

[10] Yun C K, Kahng B and Kim D, 2009 *New J. Phys.* **11** 063025
[11] Kwon S, Choi W and Kim Y, 2010 *Phys. Rev.* E **82** 021108
[12] Lee B P, 1994 *J. Phys. A: Math. Gen.* **27** 2633
[13] Täuber U C, Howard M and Lee B P, 2005 *J. Phys. A: Math. Gen.* **38** R79
[14] Leyvraz F and Redner S, 1992 *Phys. Rev.* A **46** 3132
[15] Torney D C and McConnell H M, 1983 *J. Phys. Chem.* **87** 1941
Torney D C and McConnell H M, 1983 *Proc. R. Soc. London* A **387** 147
[16] Toussaint D and Wilczek F, 1983 *J. Chem. Phys.* **78** 2642
[17] Pastor-Satorras R, Vzquez A and Vespignani A, 2001 *Phys. Rev. Lett.* **87** 258701
[18] Vázquez A, Pastor-Satorras R and Vespignani A, 2002 *Phys. Rev.* E **65** 066130
[19] Barrat A, Barthélemy M, Pastor-Satorras R and Vespignani A, 2004 *Proc. Nat. Acad. Sci.* **101** 3747
[20] Fronczak A and Fronczak P, 2009 *Phys. Rev.* E **80** 016107
[21] Einstein A, 1905 *Ann. Phys., Lpz.* **17** 549
Einstein A, 1906 *Ann. Phys., Lpz.* **19** 371
[22] Smoluchowski M, 1906 *Ann. Phys., Lpz.* **21** 756
[23] Noh J D and Rieger H, 2004 *Phys. Rev. Lett.* **92** 118701
[24] Jasch F and Blumen A, 2001 *Phys. Rev.* E **63** 041108
[25] Adamic L A, Lukose R M, Puniyani A R and Huberman B A, 2001 *Phys. Rev.* E **64** 046135
[26] Guimerá R, Díaz-Guilera A, Vega-Redondo F, Cabrales A and Arenas A, 2002 *Phys. Rev. Lett.* **89** 248701
[27] Lee S, Yook S-H and Kim Y, 2006 *Phys. Rev.* E **74** 046118
[28] Lee S, Yook S-H and Kim Y, 2007 *Physica* A **385** 743
[29] Fronczak A and Fronczak P, 2006 *Phys. Rev.* E **74** 026121
[30] Molloy M and Reed B, 1995 *Random Struct. Algorithms* **6** 161
[31] Catanzaro M, Boguñá M and Pastor-Satorras R, 2005 *Phys. Rev.* E **71** 027103
[32] Zhang Z, Zhou S, Zou T, Chen L and Guan J, 2009 *Phys. Rev.* E **79** 031110
[33] Zhang Z, Zhou S, Xie W, Li M and Guan J, 2009 *Phys. Rev.* E **80** 061111
[34] Rozenfeld H D, Havlin S and ben-Avraham D, 2007 *New J. Phys.* **9** 175
[35] Newman M E J, 2002 *Phys. Rev. Lett.* **89** 208701
[36] Barabási A-L and Albert R, 1999 *Science* **286** 509
[37] Gallos L K and Argyrakis P, 2007 *J. Phys.: Condens. Matter* **19** 065123
[38] Ben-Avraham D and Havlin S, 2000 *Diffusion and Reactions in Fractals and Disordered Systems* (Cambridge: Cambridge University Press)
[39] Tejedor V, Bénichou O and Voituriez R, 2009 *Phys. Rev.* E **80** 065104
[40] Yook S-H, Radicchi F and Meyer-Ortmanns H, 2005 *Phys. Rev.* E **72** 045105
[41] Song C, Havlin S and Makse H A, 2006 *Nature Phys.* **2** 275

J. Stat. Mech. (2011) P10001